Density-functional investigation of 3d, 4d, 5d impurity doped Au_6 clusters

Zhang Meng(张 孟), Feng Xiao-Juan(冯晓娟), Zhao Li-Xia(赵丽霞), He Li-Ming(贺黎明), and Luo You-Hua(罗有华)†

Department of Physics, East China University of Science and Technology, Shanghai 200237, *China*

(Received 18 August 2009; revised manuscript received 16 October 2009)

The general features of the geometries and electronic properties for 3d, 4d, and 5d transition-metal atom doped Au_6 clusters are systematically investigated by using relativistic all-electron density functional theory in the generalized gradient approximation (GGA). A number of structural isomers are considered to search the lowest-energy structures of M@Au_6 clusters (M=3d, 4d and 5d transition-metal atoms), and the transition metal atom locating in the centre of an Au_6 ring is found to be in the ground state for all the M@Au_6 clusters. All doped clusters, expect for Pd@Au_6, show large relative binding energies compared with a pure Au_7 cluster, indicating that doping by 3d, 4d, 5d transition-metal atoms could stabilize the Au_6 ring and promote the formation of a new binary alloy cluster.

Keywords: density functional theory, structural properties, gold clusters

PACC: 3120J, 3110, 3640

1. Introduction

The discovery of the celebrated C_{60} has aroused considerable interest in the search for highly stable metal clusters since they may be used as building blocks for novel nanomaterials.[1] In recent years, small gold clusters have attracted extensive attention due to their unique catalytic, electronic, and optical properties.[2−10] In 2008, Gruene *et al.*[11] revealed the geometries of several small neutral gold clusters in the gas phase. The geometry of Au_7 has been unambiguously assigned by comparing the experimental spectra with the calculated vibrational spectra for multiple isomers predicted by density functional theory (DFT). On the other hand, in order to enhance the stability of gold clusters and improve their chemical activities, a considerable amount of experimental and theoretical work was carried out on gold clusters doped with a transition metal (TM) atom.[12−29] Neukermans *et al.*[30] and Tanaka *et al.*[31] investigated the stability of cationic gold clusters doped with a 3d TM atom, Au_nTM^+, with TM from Sc to Zn, and extended their investigations to multiple TM atom doped gold clusters Au_NX_M clusters (X=Sc, Ti, Cr, Fe; N=1–40, M=0–3) by means of photo-fragmentation experiments.[32] Latter, Torres *et al.*[33] investigated the atomic and electronic structures of Au_nM^+ clusters (M=Sc, Ti, V, Cr, Mn, Fe, Au; $n \leq 9$) by using first-principles density functional calculations. Recently, Li *et al.*[34] studied the electronic structures and magnetic properties both experimentally and theoretically through density functional theory (DFT) calculations in a series of anionic transition-metal-doped Au clusters, M@Au_6^- (M =Ti, V, Cr). Although there are many studies of M@Au_n clusters, especially for 3d TM, most of this work has focused on anionic or cationic clusters. To our knowledge, a systematical theoretical study of 3d, 4d, 5d impurity doped Au_6 clusters has not been reported.

In our previous work,[35] the geometries, electronic and magnetic properties of the 3d transition-metal-doped gold cluster: M@Au_6 clusters (M=Sc, Ti, V, Cr, Mn, Fe, Co, Ni) were systematically studied by using the relativistic all-electron density functional theory. We found that all 3d transition-metal atoms with open d shells could stabilize the Au_6 ring structure. What are the geometric structures of 4d and 5d TM atom doped Au_6 clusters and how about the electronic properties of these clusters in 4d and 5d series? Do the situations for 4d and 5d TM atoms follow basically the same trends as those discussed for 3d impurities? Can every type of TM atom be a good way to stabilize the Au_6 by locating it in the centre of the Au_6 ring? As an effort to address the above questions, we extend our investigation to the second- and third-

†Corresponding author. E-mail: yhluo@ecust.edu.cn

© 2010 Chinese Physical Society and IOP Publishing Ltd

row transition-metal-doped Au_6 clusters and compare their results with the results of the first-row TM atom doped Au_6 clusters, thereby systematically exploring their structural and electronic properties. We describe our computational details in Section 2 and present our results and discussion in Section 3. Finally, the conclusion is given in Section 4.

2. Computational method

We perform our calculations in the present work by using the density functional theory (DFT)[36,37] implemented in the DMol^3 package.[38] The exchange-correlation interaction was treated in the generalized gradient approximation (GGA) by using the PW91 functional parametrized by Perdew and Wang.[39] All-electron spin-unrestricted calculations with scalar relativity (via VPSR tag) and a double-numerical basis set that include d polarization functions (DND) are employed in the present work. The direct inversion in iterative subspace (DIIS) approach is used to speed up SCF convergence. Considering vibrational frequency, we confirm the lowest-energy structure to be stable as the potential energy surface reaches a minimum. For more computational details, we refer readers to Ref. [35].

In order to check the validity of the computational method used for the M@Au_6 clusters, we perform the calculation on Au_2, Au_2^-, Au_7, Au_7^- and Ti@Au_6 clusters, separately, and the results are summarized in Table 1. All of the properties obtained from our calculations are in excellent agreement with available experiment data. This indicates that our methods are reliable and accurate enough to describe the structures and properties of M@Au_6 clusters.

Table 1. Calculated ground-state parameters and properties of Au_2, Au_2^-, Au_7, Au_7^- and Ti@Au_6^- clusters[a].

system	property	this work	experiment[2−11,15]
Au_2	d	2.49	2.47
	ω_e	178	191
	E_b	1.18	1.15, 1.18
	IP	9.43	9.50, 9.22
Au_2^-	d	2.587	2.582
	VDE	2.08	2.01
Au_7	ω_{e1}	168.2	165
	ω_{e2}	190.0	185
	ω_{e3}	205.5	203
Au_7^-	VDE	3.45	3.46
	ADE	3.28	3.40
Ti@Au_6^-	VDE	3.36	3.32
	ADE	3.35	3.32

[a] d: bond distance (Å, 1 Å=0.1 nm); ω_e: vibrational frequency (cm^{-1}); E_b: binding energy per atom (eV); VDE: vertical electron detachment energy (eV); ADE: adiabatic electron detachment energy (eV); IP: ionization potential (eV).

3. Results and discussion

Using the computation scheme described in Section 2, the optimized ground-state structures and two low-lying metastable isomers are obtained and shown in Fig. 1, where a big sphere refers to the impurity atom M. Here, we consider extensive two-dimensional (2D) structures and three-dimensional (3D) structures with six Au atoms surrounding a central impurity 3d atom. For a pure Au_7 cluster, a planar edge-capped triangle with C_s symmetry [see Fig. 1(b)] is found to be lowest in energy. This result is consistent with the experimental result.[11] Our calculations show that when a TM atom is doped into an Au_6 cluster, all M@Au_6 clusters prefer the ground-state 2D structure with the transition metal atom sitting in the centre of an Au_6 ring [see Fig. 1(a)].

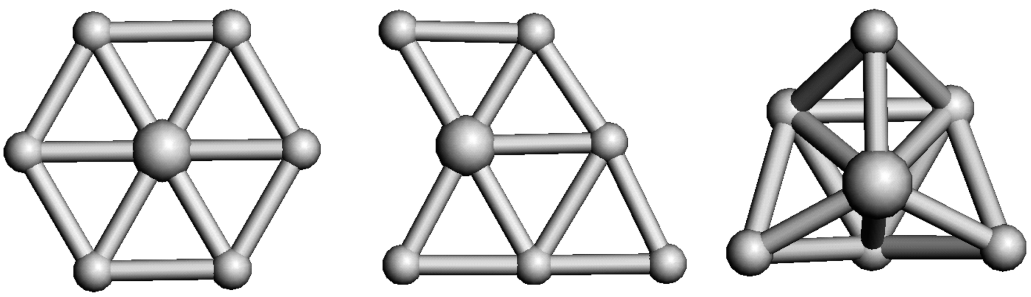


Fig. 1. Ground-state structures and low-lying isomers for M@Au_6 clusters (M=3d, 4d and 5d transition-metal atoms) obtained by using density functional theory with the PW91 functional, DND basis, and VPSR pseudopotential (see text for details). M atom is represented by big spheres.

The calculated various structural and energetic characteristics of M@Au_6 clusters are summarized in Table 2. The results for pure Au_7 clusters are also given in Table 2 for comparison. We find that the ground-state 2D structures for Mn@Au_6 cluster in 3d series form perfectly symmetrical D_{6h} structures, while Sc@Au_6, Ti@Au_6, V@Au_6, Cr@Au_6, Fe@Au_6, Co@Au_6 and Ni@Au_6 have a slight in-plane distortion due to the Jahn–Teller effect. A planar edge-capped triangle (see Fig. 1(b)) and a distorted isomer of 3D octahedral arrangement [see Fig. 1(c)] are both much higher in energy for all these clusters. In the previous work[34] of Li *et al.*, they reported that all structures of the neutral doping M@Au_6 (M=Ti, V, and Cr) clusters preferred higher symmetry than that of the pure Au_7. This is consistent with the result obtained in our work.

Table 2. Structure of M@Au_6 cluster, the optimized M–Au bond length ($R_{M-\mathrm{Au}}$), binding energy (E_b) per atom, HOMO–LUMO energy gap (E_gap), and energy separation of isomeric structure from ground-state structure (ΔE) of M@Au_6 cluster (M=3d, 4d and 5d transition-metal atoms), data on pure Au_7 cluster and relative binding energy (ΔE_b) compared with ground state Au_7. "–" means the structure is distorted and geometry optimization led to the ring structure (see Fig. 1(a)).

cluster	ground state					low-lying isomer			
	structure	$R_{M-\mathrm{Au}}$	E_b/eV	ΔE_b/eV	E_gap/eV	structure	ΔE/eV	structure	ΔE/eV
Au_7	Fig. 1(b)	2.653	2.22	0	1.08	Fig. 1(a)	0.15		
				3d series					
Sc@Au_6	Fig. 1(a)	2.660	2.75	0.53	0.22	Fig. 1(b)	0.52	Fig. 1(c)	0.58
Ti@Au_6	Fig. 1(a)	2.639	2.70	0.48	0.18	Fig. 1(b)	0.31	Fig. 1(c)	0.42
V@Au_6	Fig. 1(a)	2.626	2.52	0.30	0.12	Fig. 1(b)	0.65	Fig. 1(c)	0.68
Cr@Au_6	Fig. 1(a)	2.626	2.28	0.06	0.76	Fig. 1(b)	0.05	Fig. 1(c)	1.65
Mn@Au_6	Fig. 1(a)	2.612	2.35	0.13	0.72	Fig. 1(b)	1.83	Fig. 1(c)	2.07
Fe@Au_6	Fig. 1(a)	2.600	2.38	0.16	0.50	Fig. 1(b)	0.10	Fig. 1(c)	0.33
Co@Au_6	Fig. 1(a)	2.592	2.29	0.07	0.77	Fig. 1(b)	0.35	Fig. 1(c)	0.65
Ni@Au_6	Fig. 1(a)	2.585	2.30	0.08	0.33	Fig. 1(b)	0.26	Fig. 1(c)	0.31
				4d series					
Y@Au_6	Fig. 1(a)	2.746	2.78	0.56	2.42	Fig. 1(b)	0.54	Fig. 1(c)	0.57
Zr@Au_6	Fig. 1(a)	2.677	2.88	0.66	1.28	Fig. 1(b)	1.02	Fig. 1(b)	1.39
Nb@Au_6	Fig. 1(a)	2.655	2.69	0.47	0.90	Fig. 1(b)	0.82	Fig. 1(c)	1.13
Mo@Au_6	Fig. 1(a)	2.652	2.44	0.22	1.47	Fig. 1(b)	0.75	Fig. 1(c)	1.32
Tc@Au_6	Fig. 1(a)	2.646	2.51	0.29	1.13	Fig. 1(b)	0.76	Fig. 1(c)	1.03
Ru@Au_6	Fig. 1(a)	2.638	2.46	0.24	0.84	Fig. 1(b)	0.69	Fig. 1(c)	0.71
Rh@Au_6	Fig. 1(a)	2.641	2.33	0.11	1.01	Fig. 1(b)	0.56	Fig. 1(c)	0.75
Pd@Au_6	Fig. 1(a)	2.645	2.17	–0.05	1.10	Fig. 1(c)	0.10	Fig. 1(b)	0.37
				5d series					
Lu@Au_6	Fig. 1(a)	2.720	2.71	0.49	2.01	Fig. 1(b)	0.55	Fig. 1(c)	0.58
Hf@Au_6	Fig. 1(a)	2.646	3.04	0.82	1.21	Fig. 1(c)	1.23	Fig. 1(b)	–
Ta@Au_6	Fig. 1(a)	2.628	3.01	0.79	1.15	Fig. 1(c)	1.10	Fig. 1(b)	–
W@Au_6	Fig. 1(a)	2.624	2.76	0.54	1.00	Fig. 1(c)	1.31	Fig. 1(b)	–
Re@Au_6	Fig. 1(a)	2.639	2.50	0.28	1.41	Fig. 1(b)	0.98	Fig. 1(c)	1.37
Os@Au_6	Fig. 1(a)	2.629	2.55	0.33	0.80	Fig. 1(b)	0.86	Fig. 1(c)	1.01
Ir@Au_6	Fig. 1(a)	2.636	2.52	0.30	1.14	Fig. 1(b)	0.70	Fig. 1(c)	1.04
Pt@Au_6	Fig. 1(a)	2.630	2.42	0.20	1.05	Fig. 1(b)	0.53	Fig. 1(c)	0.92

The optimized M–Au bond length ($R_{M-\mathrm{Au}}$) of the ground-state M@Au_6 clusters for the 3d, 4d and 5d series are plotted in Fig. 2. The general features of the $R_{M-\mathrm{Au}}$ are similar in 3d, 4d and 5d series. The $R_{M-\mathrm{Au}}$ decreases with the increase of the number of d electrons except that the $R_{M-\mathrm{Au}}$ has a very slight increase from W to Pt in 5d series. Figure 2 shows that the $R_{M-\mathrm{Au}}$ of M@Au_6 clusters in 4d series is largest while it is smallest in 3d series throughout.

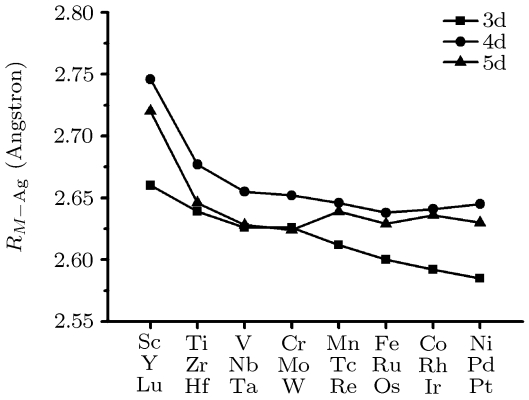


Fig. 2. Curves for bond length $R_{M-\mathrm{Au}}$ of M–Au in the ground-state M@Au_6 clusters (M=3d, 4d and 5d transition-metal atoms).

By comparing the difference ΔE_b, which is defined as the difference between the binding energy of M@Au_6 (M=3d, 4d and 5d transition-metal atoms) and the ground-state of pure Au_7 clusters in Table 2, it can be seen that the binding energy per atom for the ground-state of the M@Au_6 cluster is higher than that of pure Au_7, except for Pd@Au_6 in 4d series. This indicates that except for Pd, all doped transition metal atoms with open d shells can stabilize the Au_6 ring structure. Figure 3 gives the average binding energy of the ground-state M@Au_6 clusters. As we can see from Fig. 3, the largest relative binding energy per atom compared with pure Au_7 appears at Hf with 0.82 eV. So, Hf@Au_6 should be the most stable among these clusters.

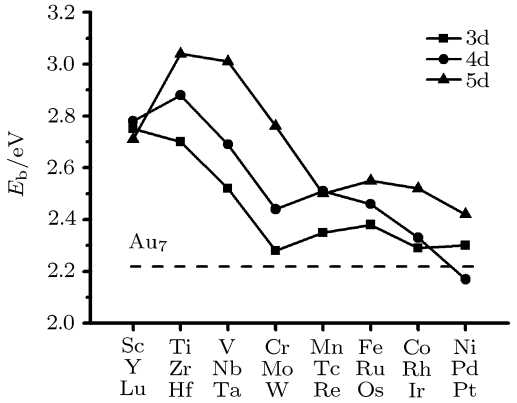


Fig. 3. Curves for average binding energy (E_b) of the ground-state M@Au_6 clusters (M=3d, 4d and 5d transition-metal atoms). The horizontal dot line is for the pure Au_7 cluster.

The highest occupied molecular orbital–lowest occupied molecular orbital (HOMO–LUMO) energy gap is another useful quantity for examining the kinetic stability of clusters. In the present paper, the HOMO–LUMO is calculated for all spin branches. Figure 4 gives the values of E_gap of 3d, 4d, 5d impurities doped in the Au_6 ring. The values of E_gap for all 3d impurity doped Au_6 clusters are remarkably smaller than that of pure Au_7. We compare the values of E_gap of all M@Au_6 clusters and find that the E_gap of the Y@Au_6 cluster (2.42 eV) is the largest, 1.34 eV larger than the E_gap of the pure Au_7 cluster. This suggests that Y@Au_6 is chemically more stable than the neighbouring clusters. On the other hand, V@Au_6 has the smallest value of E_gap, only 0.12 eV. From the above discussion, we can conclude that although doping the TM atom can enhance the structural stability of gold clusters, the kinetic stabilities of these transition-metal doped clusters are very variable when doped with different TM atoms.

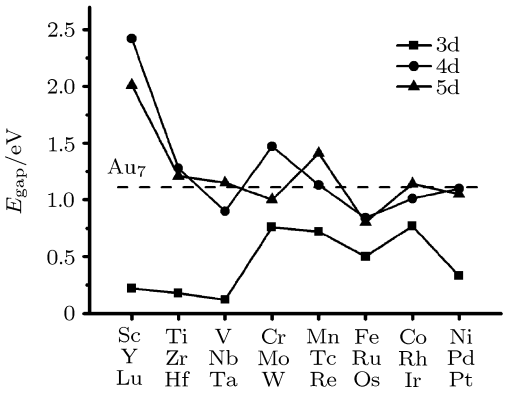


Fig. 4. Curves for HOMO–LUMO energy gap (E_gap) of the ground-state M@Au_6 clusters (M=3d, 4d and 5d transition-metal atoms). The horizontal dot line is for the pure Au_7 cluster.

4. Conclusion

We systematically investigated the geometries and the electronic properties of 3d, 4d, and 5d impurity doped Au_6 clusters by using relativistic all-electron density functional theory in the generalized gradient approximation. Many isomers are found and three representative structures are given and discussed. For all the M@Au_6 clusters (M=3d, 4d and 5d transition-metal atoms), the most stable structure is a 2D structure with the transition metal atom sitting in the centre of an Au_6 ring. Except for Pd@Au_6, all doped clusters show large relative binding energies compared with a pure Au_7 cluster, indicating that transition-metal atoms with open d shells can stabilize the Au_6 ring structure. This suggests that the stable M@Au_6 guest–host bimetallic clusters may have potential utility in new nanomaterials as building blocks.

References

[1] Kroto H W, Heath J R, O'Brien S C, Curl R F and Smalley R E 1985 *Nature* **318** 162

[2] Huber K P and Herzberg G 1979 *Constants of Diatomic Molecules* (New York: Van Nostrand Reinhold)

[3] Simard B and Hackett P A 1990 *J. Mol. Spectrosc.* **142** 310

[4] Ho J, Ervin K and Lineberger W 1990 *J. Chem. Phys.* **93** 6987

[5] Taylor K, Pettitte-Hall C, Cheshnovsky O and Smalley R 1992 *J. Chem. Phys.* **96** 3319

[6] Jackschath C, Rabin I and Schulze W 1992 *Ber. Bunsenges. Phys. Chem.* **96** 1200

[7] Barnett R N, Cleveland C I, Häkkinen H, Luedtke W D, Yamouleas C and Landsman U 1999 *Eur. Phys. J.* D **9** 95

[8] Häkkinen H, Yoon B, Landman U, Li X, Zhai H J and Wang L S 2003 *J. Phys. Chem.* A **107** 6168

[9] Fernández E M, Soler J M, Garzón I L and Balbás L C 2004 *Phys. Rev.* B **70** 165403

[10] Mao H P, Wang H Y, Ni Y, Xu G L, Ma M Z, Zhu Z H and Tang Y J 2004 *Acta Phys. Sin.* **53** 1766 (in Chinese)

[11] Gruene P, Rayner D M, Redlich B, van der Meer A F G, Lyon J T, Meijer G and Fielicke A 2008 *Science* **321** 674

[12] Chen M X and Yan X H 2008 *J. Chem. Phys.* **128** 174305

[13] Pyykkö P and Runeberg N 2002 *Angew. Chem. Int. Ed.* **41** 2174

[14] Fa W and Dong J M 2008 *J. Chem. Phys.* **128** 144307

[15] Wang L M, Bulusu S, Huang W, Pal R, Wang L S and Zeng X C 2007 *J. Am. Chem. Soc.* **129** 15136

[16] Tanaka H, Neukermans S, Janssens E, Silverans R E and Lievens P 2003 *J. Am. Chem. Soc.* **125** 2862

[17] Janssens E, Tanaka H, Neukermans S, Silverans R E and Lievens P 2003 *New J. Phys.* **5** 46

[18] Yamada Y and Castleman Jr A W 1992 *J. Chem. Phys.* **97** 4543

[19] Sun Q, Gong X G, Zheng Q Q, Sun D Y and Wang G H 1996 *Phys. Rev.* B **54** 10896

[20] Wang H Y, Li X B, Tang Y J, King R B and Schaefer H F 2007 *Chin. Phys.* **16** 1660

[21] Van De Walle J, Tarento R J and Joyes P 1999 *Surf. Rev. Lett.* **6** 307

[22] Bouwen W, Vanhoutte F, Despa F, Bouckaert S, Neukermans S, Kuhn L T, Weidele H, Lievens P and Silverans R E 1999 *Chem. Phys. Lett.* **314** 227

[23] Heinebrodt M, Malinowski N, Tast F, Branz W, Billas I M L and Martin T P 1999 *J. Chem. Phys.* **110** 9915

[24] Koyasu K, Mitsui M, Nakajima A and Kaya K 2002 *Chem. Phys. Lett.* **358** 224

[25] Chen X, Peng X, Deng K M, Xiao C Y, Hu F L and Tan W S 2009 *Acta Phys. Sin.* **58** 5370 (in Chinese)

[26] Wang S Y, Yu J Z, Mizuseki H, Sun Q, Wang C Y and Kawazoe Y 2004 *Phys. Rev.* B **70** 165413

[27] Li X, Kiran B, Li J, Zhai H J and Wang L S 2002 *Angew. Chem. Int. Ed.* **41** 4786

[28] Häkkinen H, Abbet S, Sanchez A, Heiz U and Landman U 2003 *Angew. Chem. Int. Ed.* **42** 1297

[29] Zhao L X, Feng X J, Cao T T, Liang X and Luo Y H 2009 *Chin. Phys.* B **18** 2709

[30] Neukermans S, Janssens E, Tanaka H, Silverans R E and Lievens P 2003 *Phys. Rev. Lett.* **90** 033401

[31] Tanaka H, Neukermans S, Janssens E, Silverans R E and Lievens P 2003 *J. Chem. Phys.* **119** 7115

[32] Janssens E, Tanaka H, Neukermans S, Silverans R E and Lievens P 2004 *Phys. Rev.* B **69** 085402

[33] Torres M B, Fernández E M and Balbás L C 2005 *Phys. Rev.* B **71** 155412

[34] Li X, Kiran B, Cui L F and Wang L S 2005 *Phys. Rev. Lett.* **95** 253401

[35] Zhang M, He L M, Zhao L X, Feng X J and Luo Y H 2009 *J. Phys. Chem.* C **113** 6491

[36] Ordejón P, Artacho E and Soler J M 1996 *Phys. Rev.* B **53** R10441

[37] Sánchez-Portal D, Ordejón P, Artacho E and Soler J M 1997 *Int. J. Quantum Chem.* **65** 453

[38] Delley B 1990 *J. Chem. Phys.* **92** 508

[39] Perdew J P and Wang Y 1992 *Phys. Rev.* B **45** 13244